University of Kurdistan
Dept. of Electrical and Computer Engineering
Smart/Micro Grid Research Center
smgrc.uok.ac.ir

Event-Triggered Voltage Control of Inverter- Based Microgrids

Babak Abdolmaleki, Alireza Seifi, Mohammad Mehdi Arefi, and Qobad Shafiee

Published (to be published) in: Proceedings of the 9th IEEE conference on Power Electronics, Drives Systems and Technologies, PEDSTC 2018

(Expected) publication date: 2018

Citation format for published version:

B. Abdolmaleki, A. Seifi, M. M. Arefi, and Q. Shafiee, ‘‘Event-Triggered Voltage Control of Inverter-Based Microgrids,’’ In Proc. 9th IEEE Power Electronics, Drives Systems, and Technologies Conference (PEDSTC 2018), Tehran, Iran, Feb. 2018, pp. 522-528.

Event-Triggered Voltage Control of Inverter-Based Microgrids

Babak Abdolmaleki, Alireza Seifi, and Mohammad Mehdi Arefi
M.Sc. Graduate, Professor, and Associate Professor
School of Electrical and Computer Engineering
Shiraz University, Shiraz, Iran
abdolmaleki.p.e@gmail.com, seifi@shirazu.ac.ir,
arefi@shirazu.ac.ir

Qobad Shafiee
Assistant Professor
Smart/Micro Grids Research Center (SMGRC)
Department of Electrical Engineering
University of Kurdistan, Sanandaj, Iran
q.shafiee@uok.ac.ir

***Abstract*—This paper proposes a secondary voltage control for inverter-based microgrids (MGs) using event-triggered communications. In the proposed method, state equations of the MG are transferred into a multi-agent system with single integrator dynamics using the feedback linearization technique. Then, considering the allowable range of voltages, a leader-following tracking control is designed such that the voltages of all the distributed generations (DGs) converge to a reference voltage. This reference is generated by using a critical bus voltage controller which is only available in a few DGs. The controller is designed for both continuous and event-triggered communications. The latter scheme, uses an event-triggering mechanism under which, the system remains L_2-stable and inter-event times are always positive. The effectiveness of the proposed controller is validated by numerical simulation for a test MG in the MATLAB/Simulink environment.**

Keywords—Event-triggered control, L_2-stability, Leader-following tracking control, Microgrid, Secondary control.

I. INTRODUCTION

Compensation for voltage deviation caused by droop-control is one of the main tasks in the secondary control of AC microgrids (MGs) [1]. Secondary control relies on communication network; therefore, distributed schemes using sparse communication networks are preferred to centralized architectures [2]. Recently, leader-following tracking synchronization algorithms have been widely investigated for voltage and frequency regulation of MGs (e.g., see [3] and references therein). The existing works are mostly developed based on continuous communications, while realistic communication infrastructures are not continuous and usually have limited bandwidth [4].

Event-triggered control is a strategy in which the control rule is updated only when measurement error of a decision variable violates a specific threshold. This control strategy leads to more efficient usage of communication medium in networked control systems [5].

Event-triggered control of power systems has been already introduced in the literature [6]–[10]. An event-triggered load frequency control for power systems is proposed in [6], where an event-triggering mechanism guarantees boundedness of the closed-loop system. In [7], a fully distributed event-triggered load sharing mechanism is proposed. In this work, average-consensus algorithm is used to control the active powers of DGs coordinately via controlling their output currents. A distributed reactive power sharing control with event-triggered communications is proposed in [8], where a new communication-based nonlinear algorithm is proposed providing proper reactive power sharing between DGs by changing their output voltages. Similarly, a droop-free event-triggered current sharing scheme for converter-based DC MGs is proposed in [9]. In [10], a coordinated control is proposed to control the active power sharing among the interconnected DC and AC MGs. In this control strategy, an event-triggered consensus-based control strategy is proposed to achieve consensus. None of these works investigates cooperative voltage control of the DGs in AC MGs.

Distributed secondary voltage control of MGs resembles tracking synchronization of multi-agent systems [3]. Event-triggered leader-following tracking control of multi-agent systems is deeply investigated in [11]. Under the proposed event-triggering mechanism, tracking errors of the follower agents and inter-event times are upper- and lower-bounded, respectively.

In this paper, we develop a state-space model for droop-controlled MGs. To shift the droop characteristics along the voltage axis, a secondary control variable is added to the conventional droop mechanism. By using feedback linearization technique, the state-space model is transferred to a multi-agent system with single-integrator dynamics. A leader-following tracking synchronization algorithm is then used to restore the output voltages of all DGs to a time-varying reference voltage. The reference voltage generator is an integral control which tries to reduce the error between critical bus voltage and the nominal voltage, while maintaining the DG voltages in an allowable range. The control scheme is developed for both continuous and event-triggered communications. In the event-triggered scheme, an event is detected as soon as a function of measurement error associated with local voltage, violates a predefined threshold. It is shown that under specific circumstances, the controlled MG system is L_2-stable. In addition, we show that inter-event times associated with all DGs are lower positive bounded. Finally, effectiveness of the proposed control schemes is validated by using numerical simulations in

978-1-5386-4699-1/18/$31.00 ©2018 IEEE

MATLAB/Simulink environment. Throughout the paper, $\mathbb{R}^n$ denotes *n*-dimensional vector space over the field of real numbers and $\mathbb{R}^{n\times m}$ denotes the space containing all the real matrices with *n* rows and *m* columns.

The rest of this paper is organized as follows. Section II provides the microgrid's system modelling. The proposed secondary controller design is provided in section III. To verify the effectiveness of the proposed control scheme, numerical simulations are included in section IV. Section V concludes the paper.

II. System Modelling

Fig. 1 depicts a hierarchical control scheme for islanded MGs. The scheme consists of three layers: communication, physical, and control layers.

A. Communication Layer [3], [11]

The MG communication network can be regarded as a directed graph (digraph) with DGs and communication links as its nodes and edges, respectively. Consider the digraph $G=(N_G,E_G,\mathbf{A}_G)$, where $N_G=\{1,...,n\}$, $E_G=N_G\times N_G$, and $\mathbf{A}_G=[a_{ij}]\in\mathbb{R}^{n\times n}$ are its node set, edge set, and adjacency matrix, respectively. If node *i* can receive information from node *j*, then node *j* is a neighbor of node *i*, $(j,i)\in E_G$, and $a_{ij}>0$, otherwise node *j* is not a neighbor of node *i*, $(j,i)\notin E_G$, and $a_{ij}=0$. We assume $(i,i)\notin E_G$, and $a_{ii}=0$. Let $N_i=\{j\,|\,(j,i)\in E\}$ and $d_i=\sum_{j\in N_i}a_{ij}$ be the neighbor set and *in-degree* of node *i*, respectively. $\mathbf{L}=\mathbf{D}-\mathbf{A}$ is then *Laplacian* matrix of digraph *G*, where $\mathbf{D}=diag\{d_i\}\in\mathbb{R}^{n\times n}$. Let $\mathbf{B}=diag\{b_i\}\in\mathbb{R}^{n\times n}$, where $b_i>0$ if node *i* can reach the node 0 (called the *leader*) and $b_i=0$, otherwise. A *direct path* from node *i* to node *j* is a sequence of pairs belong to *E* expressed as $\{(j,t_1),(t_1,t_2),...,(t_m,i)\}$. A digraph has a *spanning tree*, if there is a node *r* (called the *root*) such that, there is a direct path from the root to any other node.

B. Physical and Control Layers

These layers are depicted in Fig. 2. Each DG comprises a

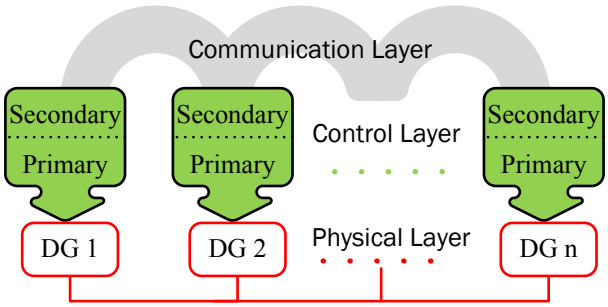

Fig. 1. Hierarchical controlled microgrid.

voltage sourced inverter (VSI), a voltage controlled oscillator (VCO), a LCL filter, a VSI's output current controller, a capacitor's voltage controller, an average power measurement block, and a droop-control unit. Details on design of mentioned parts are provided in [12]. Voltage and current controllers are normally designed in the way that the subsystem comprising these controllers and their corresponding blocks (VSI and LC filter) has a high bandwidth (BW) (e.g. BW>0.2 kHz), whereas power measurement filters are very slow (e.g. with BW<10 Hz). Therefore, neglecting the dynamics of mentioned subsystem, one can consider each DG as a droop-controlled voltage source (DCVS) which is connected to the rest of MG through a connector [13]. Let $\delta_i,\omega_i,V_i,P_i$, and Q_i be phase angle, frequency, and magnitude of output voltage and measured active and reactive powers of i^{th} DCVS, respectively. Accordingly, the state-space model for the whole MG system consisting of *n* DGs can be expressed as

$$\begin{aligned}&\dot{\delta}_i=\omega_i-\omega_{com},\\&\dot{P}_i=-\omega_{cut}P_i+\omega_{cut}\tilde{P}_i,\\&\dot{Q}_i=-\omega_{cut}Q_i+\omega_{cut}\tilde{Q}_i,\\&\omega_i=\omega_{nom}-m_iP_i,\ V_i=V_{nom}-n_iQ_i,\ i=1,...,n,\end{aligned}\tag{1}$$

where $\omega_{com},\omega_{nom},V_{nom},\omega_{cut},m_i$, and n_i are common frequency, nominal frequency, nominal voltage magnitude, power measurement filters' cutoff frequency, and droop coefficients, respectively. $\tilde{P}_i$ and $\tilde{Q}_i$ are active and reactive powers, respectively. In droop-controlled MG, while the DGs' powers are shared properly, droop mechanism causes steady-state deviations in DGs' output voltages. To compensate for these deviations, let us introduce secondary

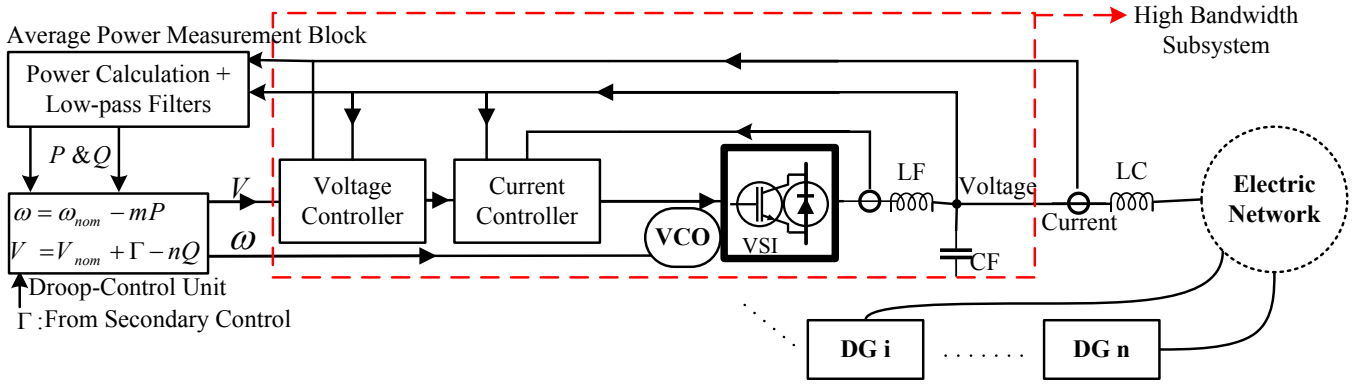

Fig. 2. Physical and control layers of microgrid.

control variable Γ_i with the following implementation

$$\begin{aligned} \dot{\Gamma}_i &= u_{V_i}, \\ V_i &= V_{nom} + \Gamma_i - n_i Q_i, \quad i = 1,...,n, \end{aligned} \tag{2}$$

where $u_{V_i} \in \mathbb{R}$ are secondary control inputs associated with Γ_i. Our aim is to shift the (V-Q) droop-control characteristics along voltage axis so that:

$$[V_i, V_c]^T \rightarrow [V_{ref}, V_{cref}]^T, \quad \forall i, \tag{3}$$

where V_c and V_{cref} are critical bus voltage and its reference value, respectively. Therefore, we can reformulate the state-space equations of the MG system as

$$\begin{aligned} \dot{\mathbf{x}}_\mathbf{i} &= f_i(\mathbf{x_i}, \mathbf{x_j}, u_{V_i}), \\ y_i &= V_i, \quad i, j = 1,...,n, \end{aligned} \tag{4}$$

where $\mathbf{x_i} = [\delta_i, P_i, Q_i, \Gamma_i]^T \in \mathbb{R}^4$ and $y_i \in \mathbb{R}$ are state and output vectors, respectively. It should be noted some $f_i : \mathbb{R}^{4n+1} \rightarrow \mathbb{R}^4$, can be obtained by using (1), (2), and power flow equations of electrical network (e.g., see [13]).

III. Secondary Control Design

A. Preliminaries

According to the feedback linearization mechanism [14], the input vector u_{V_i} appears after differentiating y_i, i.e.,

$$\dot{y}_i = u_{V_i} - n_i \dot{Q}_i, \quad i = 1,...,n. \tag{5}$$

Let us define the auxiliary input vector $U_i = \dot{y}_i$. Substituting this vector for $\dot{y}_i$ in (5) yields

$$u_{V_i} = U_i + n_i \dot{Q}_i, \quad i = 1,...,n. \tag{6}$$

The above feedback linearization procedure transforms the nonlinear dynamics of each DG in (4) to a single integrator dynamic below and a set of stable internal dynamics [15].

$$\dot{y}_i = U_i \in \mathbb{R}. \tag{7}$$

Thanks to the use of feedback linearization technique, we can consider MG system as a multi-agent system with single integrator dynamics (7). To achieve the control aim in (3), it is sufficient to find appropriate U_i and $y_{ref} = V_{ref}$, such that $y_i \rightarrow y_{ref}, \forall i$, and $V_c \rightarrow V_{cref}$.

Definition 1 [16]: A linear system is said to be finite-gain *L_2-stable* from the disturbance $\boldsymbol{\psi}$ to state variable $\mathbf{z}$ with an *induced gain* less than μ if there exists constants $\mu, \eta > 0$ such that if $\|\boldsymbol{\psi}\| \le \alpha$ then,

$$\sqrt{\int_{t_0}^{\infty} \|\mathbf{z}\|^2 dt} \le \mu \sqrt{\int_{t_0}^{\infty} \|\boldsymbol{\psi}\|^2 dt} + \eta, \tag{8}$$

where $\|.\|$ denotes the Euclidian 2-norm.

Definition 2 [15]: A matrix is *Hurwitz stable*, if the real part of all its *eigenvalues* are negative.

Definition 3 [16]: The *symmetric* matrix $\mathbf{P}$ is *positive definite*, if for the nonzero column vector $\mathbf{x}$, the scalar $\mathbf{x}^T\mathbf{P}\,\mathbf{x}$ is positive.

Definition 4: A square matrix is said to be *nonsingular* if it has nonzero determinant.

Lemma 1 [17]: If the leader node in diagraph G is *globally reachable* i.e., there exist a *spanning tree* rooted at node r which is pinned to the leader $(b_r = 1)$, then the matrix $(-\mathbf{M})$ is *nonsingular*, *Hurwitz stable* and there exists a *positive definite* matrix $\mathbf{P}$ such that $\mathbf{H} = \mathbf{PM} + \mathbf{M}^T\mathbf{P} > \mathbf{0}$, where $\mathbf{M} = \mathbf{L} + \mathbf{B}$, $\mathbf{F} = \mathbf{PMM}^T\mathbf{P}$, and $\mathbf{R} = \mathbf{M}^T\mathbf{M}$.

Lemma 2 [16]: If $\mathbf{P}$ is *positive definite*, then:

$$\lambda_m^{\mathbf{P}} \mathbf{x}^T\mathbf{x} \le \mathbf{x}^T\mathbf{P}\mathbf{x} \le \lambda_M^{\mathbf{P}} \mathbf{x}^T\mathbf{x}, \tag{9}$$

where $\lambda_m^{\mathbf{P}}$ and $\lambda_M^{\mathbf{P}}$ are the smallest and largest eigenvalues of $\mathbf{P}$, respectively.

B. Proposed Controller with Continuous Communications

Once DGs communicate with each other through diagraph G, described in section (II-A), we can achieve the aim in (3) by using leader-following tracking control with an active leader. Accordingly, the system (7) with the proposed control scheme is as follows

$$\begin{aligned} &\dot{\Gamma}_c = k_c(V_{cref} - V_c), \\ &y_{ref} = V_{nom} + \Gamma_c, \quad |\Gamma_c| < 0.05V_{nom}, \\ &\dot{y}_i = kz_i, \\ &z_i = \sum_{j \in N_i} a_{ij}(y_j - y_i) + b_i(y_{ref} - y_i), \quad \forall i, j, \end{aligned} \tag{10}$$

where $k > 0$ is feedback gain and $k_c > 0$, is integral gain of critical bus voltage controllers. Γ_c is the critical bus voltage control variable for changing the V_{ref}. In order for DGs voltages not to violate the allowable range ($\pm 1.05V_{nom}$), this variable is limited.

Proposition 1. Suppose DGs in the MG (4) communicate with each other through diagraph G. If reference voltage V_{ref} is *globally reachable* (***Lemma 1*** holds), then subject to the proposed controllers in (10), the system (7) and consequently (4) achieve the control aim in (3) with zero steady-state error.

Proof. Global representation of (10) is

$$\begin{aligned} \dot{\Gamma}_c &= k_c(V_{cref} - V_c), \\ \dot{\mathbf{y}} &= k\mathbf{M}\left(y_{ref}\mathbf{1_n} - \mathbf{y}\right), \end{aligned} \tag{11}$$

where $\mathbf{y} = [y_1, ..., y_n]^T$ and $\mathbf{1_n} \in \mathbb{R}^n$ are global state vector and vector of ones, respectively.

According to (11), in the steady-state, V_c converges to V_{cref} with a small error so that y_{ref} takes a constant value, thus

$$\dot{\mathbf{y}} = k\mathbf{M}\left(y_{ref}\mathbf{1_n} - \mathbf{y}\right) = 0 \times \mathbf{1_n}. \tag{12}$$

Now, if ***Lemma 1*** holds i.e., $\mathbf{M}$ is nonsingular, then $V_i = V_{ref}, \forall i$. This completes the ***Proof***. ■

C. Proposed Controller with Event-Triggered Communications

To reduce the communications between DGs, we are looking for a control scheme in which, i^{th} DG sends data to communication network only at its own event times. Let $t_0^i, t_1^i, ...,$ denote i^{th} DG event times. Accordingly, we

propose the following control scheme for system (7) and the same reference generator dynamics as in (10).

$$\begin{aligned}\dot{y}_i &= k\tilde{z}_i(t),\ \ t\in[t^i_{k_i},t^i_{k_i+1}),\\ \tilde{z}_i &= \sum_{j\in N_i} a_{ij}(y_j(t^j_{k_j})-y_i(t^i_{k_i}))\\ &\quad + b_i(y_{ref}(t^r_{k_r})-y_i(t^i_{k_i}),\ \ \forall i,j\end{aligned} \tag{13}$$

where $y_i(t^i_{k_i})$, $y_j(t^j_{k_j})$, and $y_{ref}(t^r_{k_r})$ are the last stored sampled output vectors of i^{th} and j^{th} DGs and reference generator, respectively. These vectors are held constant during time intervals $t\in[t^i_{k_i},t^i_{k_i+1})$, $t\in[t^j_{k_j},t^j_{k_j+1})$, and $t\in[t^r_{k_r},t^r_{k_r+1})$, respectively. It should be noted that $y_j(t^j_{k_j})$ and $y_{ref}(t^r_{k_r})$ may vary during time interval $t\in[t^i_{k_i},t^i_{k_i+1})$.

Let $e_i(t)=y_i(t^i_{k_i})-y_i(t)$ be the measurement error of y_i. Therefore, local combinational measurement errors for $t\in[t^i_{k_i},t^i_{k_i+1})$ are as follows

$$\begin{aligned}s_i(t)&=\tilde{z}_i(t)-z_i(t)\\ &=\sum_{j\in N_i} a_{ij}(e_j(t)-e_i(t))+b_i(e_{ref}(t)-e_i(t)).\end{aligned} \tag{14}$$

Substituting (14) to (13) yields

$$\dot{y}_i(t)=kz_i(t)+ks_i(t),\ \ t\in[t^i_{k_i},t^i_{k_i+1}). \tag{15}$$

We are looking for an event-triggering mechanism under which the system (13) with the proposed control scheme remains stable and the control aim in (3) is achieved with a desired nonzero steady-state error. In addition, the time between any two consecutive event-times is lower positive bounded. Our proposed event-triggering mechanism is as follows

$$\begin{aligned}t^i_{k_i+1}&=\inf\{t>t^i_{k_i}:f_{e_i}=2\tau\lambda^{\mathbf{R}}_M e_i^2>\gamma_i\},\\ t^r_{k_r+1}&=\inf\{t>t^r_{k_r}:f_{e_r}=2\tau\lambda^{\mathbf{R}}_M e_{ref}^2>\gamma_r\}.\end{aligned} \tag{16}$$

where inf{.} denotes the greatest element in {.} that is less than or equal to all elements of {.}

Proposition 2. Suppose DGs in the MG (4) communicate with each other through diagraph G. If reference voltage V_{ref} is *globally reachable* (***Lemma 1*** holds) and local vectors $y_i(t^i_{k_i})$, and $y_{ref}(t^r_{k_r})$ are sampled and broadcasted at event-times (16), then subject to the proposed controllers in (10) and (13), the system (7) and consequently (4) are L_2-*stable*. Accordingly, the control aim in (3) is achieved with a nonzero desired steady-state error.

Proof. Global representation of (15) in terms of combinational variables and considering the dynamics of reference generator is

$$\begin{aligned}\dot{y}_{ref}&=k_c(V_{cref}-V_c),\\ \dot{\mathbf{z}}&=-k\mathbf{M}\mathbf{z}-k\mathbf{M}\mathbf{s}+\mathbf{M}(\dot{y}_{ref}\mathbf{1_n}),\end{aligned} \tag{17}$$

where

$$\begin{aligned}&\mathbf{z}=[z_1,...,z_n]^T=\mathbf{M}(y_{ref}\mathbf{1_n}-\mathbf{y}),\mathbf{e}=[e_1^T,...,e_n^T]^T\\ &\mathbf{s}=[s_1,...,s_n]^T=\mathbf{M}(e_{ref}\mathbf{1_n}-\mathbf{e}).\end{aligned} \tag{18}$$

Considering the *Lyapunov candidate* $E=\mathbf{z}^{\mathbf{T}}\mathbf{P}\mathbf{z}$, one can write

$$\dot{E}=\dot{\mathbf{z}}^{\mathbf{T}}\mathbf{P}\mathbf{z}+\mathbf{z}^{\mathbf{T}}\mathbf{P}\dot{\mathbf{z}}. \tag{19}$$

Using ***Lemma 1***, ***Lemma 2***, (17), (18), and the inequality $\pm 2\mathbf{x}^T\mathbf{y}\le\tau\mathbf{x}^T\mathbf{x}+\tau^{-1}\mathbf{y}^T\mathbf{y},\forall\tau>0$, it follows from (19) that:

$$\begin{aligned}\dot{E}&\le -k\overbrace{(\lambda^{\mathbf{H}}_m-2\tau^{-1}\lambda^{\mathbf{F}}_M)}^{\sigma}\mathbf{z}^T\mathbf{z}+2nk\tau\lambda^{\mathbf{R}}_M e_{ref}^2\\ &\quad+2k\tau\lambda^{\mathbf{R}}_M\mathbf{e}^T\mathbf{e}+n\tau k^{-1}\dot{y}_{ref}^2,\end{aligned} \tag{20}$$

where $\tau=4\lambda^{\mathbf{F}}_M/\lambda^{\mathbf{H}}_m$ and n is the number of DGs. $\mathbf{P},\mathbf{H},\mathbf{F},\mathbf{R},\lambda_m$, and λ_M are introduced in ***Lemma 1*** and ***Lemma 2***. Now, considering the event trigger mechanism in (16), one can write

$$\begin{aligned}\frac{\dot{E}}{k}&\le-\sigma\mathbf{z}^T\mathbf{z}+\frac{\overbrace{(\dot{y}_{ref}^2+k^2n^{-1}\tau^{-1}(n\gamma_r+\sum_i^n\gamma_i))}^{\beta^2}}{k^2n^{-1}\tau^{-1}}\\ &\le-\sigma\mathbf{z}^T\mathbf{z}+k^{-2}n\tau\boldsymbol{\psi}^T\boldsymbol{\psi},\end{aligned} \tag{21}$$

where, $\boldsymbol{\psi}=[\dot{y}_{ref},\beta]^T$, $\boldsymbol{\psi}^T\boldsymbol{\psi}\le\alpha(t)<\bar{\alpha}$.

Integrating (21) yields

$$\frac{E}{k}+\sigma\int_0^t\mathbf{z}^T\mathbf{z}dt\le k^{-2}n\tau\int_0^t\boldsymbol{\psi}^T\boldsymbol{\psi}dt+\frac{E_0}{k}, \tag{22}$$

which implies that the system is L_2-*stable* from $\boldsymbol{\psi}$ to $\mathbf{z}$ with *induced gain* less than $\sqrt{k^{-2}n\tau/\sigma}$. Let multiply (21) by kE/E, then from ***Lemma 2*** we have that:

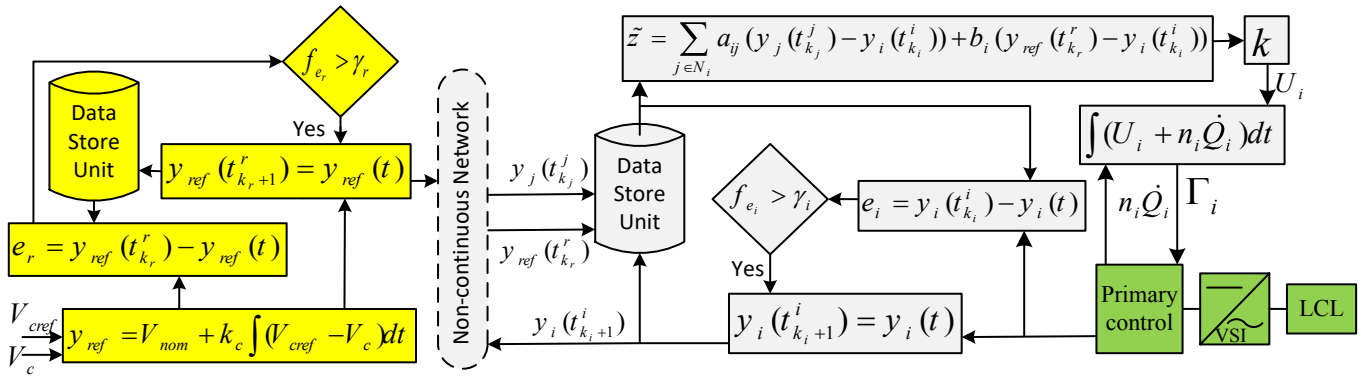

Fig. 3. Schematic diagram of the proposed controller (*proposition 2*); greens are physical and control layers explained in section II-B, grays are event-triggered secondary controller associated with i^{th} DG, yellows are critical bus voltage controller and its event-triggering mechanism.

$$\dot{E} \le -\frac{k\sigma}{\lambda_M^{\mathbf{P}}} E + k^{-1} n\tau\alpha. \tag{23}$$

Integrating (23) yields

$$E \le E_0 e^{-\frac{k\sigma}{\lambda_M^P} t} + k^{-1} n\tau \int_0^t e^{-\frac{k\sigma}{\lambda_M^P}(t-\xi)} \alpha(\xi) d\xi, \tag{24}$$

By using ***Lemma 2***, in the steady-state $(t \to \infty, \dot{y}_{ref} = 0)$, one can conclude that:

$$\limsup_{t\to\infty} \mathbf{z}^T \mathbf{z} \le \frac{\lambda_M^{\mathbf{P}} (n\gamma_r + \sum_i^n \gamma_i)}{(\sigma\lambda_m^{\mathbf{P}})}. \tag{25}$$

By using (25) and ***Lemma 2*** it further implies that:

$$\limsup_{t\to\infty} \sum_i^n (V_{ref} - V_i)^2 \le \frac{\lambda_M^{\mathbf{P}} (n\gamma_r + \sum_i^n \gamma_i)}{\sigma\lambda_m^{\mathbf{P}} \lambda_m^{\mathbf{R}}} = \Delta > 0. \tag{26}$$

This confirms, V_i converges to the reference value with a nonzero steady-state error. Next, we will show the inter-event times are lower positive bounded. Using $\pm 2\mathbf{x}^T \mathbf{y} \le \tau \mathbf{x}^T \mathbf{x} + \tau^{-1} \mathbf{y}^T \mathbf{y}, \forall \tau > 0$ and considering the function f_{e_i} in (16), we have

$$\dot{f}_{e_i} \le \rho f_{e_i} + \underbrace{2\tau\lambda_M^{\mathbf{R}} \rho^{-1} \dot{y}_i^2}_{\theta(t)}, \quad \rho > 0. \tag{27}$$

Therefore, for initial condition $\phi_i(t_{k_i}^i) = f_{e_i}(t_{k_i}^i) = 0$ and $t \in \left[t_{k_i}^i, t_{k_i+1}^i\right)$, it can be written that:

$$f_{e_i} \le \phi_i(t) = \int_{t_{k_i}^i}^t e^{\rho(t-\xi)} \theta(\xi) d\xi. \tag{28}$$

Next event-time $t_{k_i+1}^i$, is when $\phi_i(t) > \gamma_i > 0$. Therefore, $\phi_i(t)$ takes a finite time $t_{k_i+1}^i$, to grow from zero to the positive value γ_i; thus, the inter-event time $(t_{k_i+1}^i - t_{k_i}^i)$, is always positive. Similar reasoning is valid for other DGs and reference generator, as well. This completes the ***Proof***. ■

The general scheme of proposed method is shown in Fig. 3.

Remark 1: Herein, the frequencies and active powers of DGs are controlled by conventional droop-control. In addition, the variation of voltage has negligible impact on the frequency control i.e., frequency and voltage droop-controllers are highly decoupled.

Remark 2: It should be noted that the reactive power sharing and voltage regulation are two conflicted objectives; therefore, in this paper we just investigate the voltage regulation objective.

IV. Case Studies

An islanded radial MG (220 V, 50Hz) consisting of four DGs is simulated in the MATLAB/Simulink environment, to verify the effectiveness of the proposed controllers. Fig. 4 depicts the different layers of the MG, where the electrical and control parameters of DGs, loads, and transmission lines are also given. Herein, the PCC bus is considered as the critical bus and its voltage should remain as close as possible to the nominal voltage. The simulations consist of four stages for all the case studies:

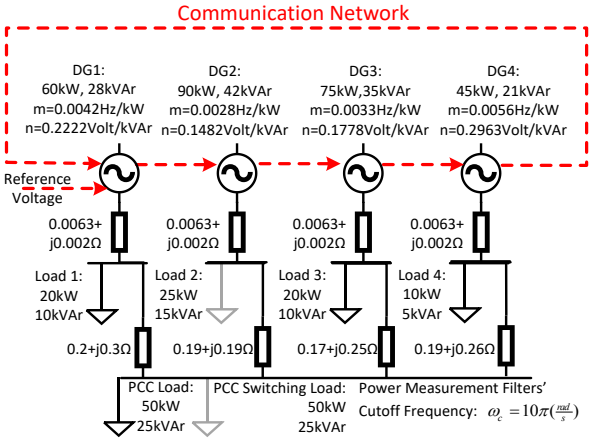

Fig. 4. Microgrid test system and its specifications.

Stage 1. (*0-1s*): The MG is controlled by droop-control.

Stage 2. (*1-4s*): Proposed secondary control is activated at *t=1s*.

Stage 3. (*4-7s*): The PCC load is doubled at *t=4s*.

Stage 4. (*7-10s*): The added load to the PCC load in the former stage and load 2 are switched off at *t=7s*.

We assume $\gamma_i = \gamma_r, \forall i$. Some of required matrices and parameters are

$$\mathbf{P} = \begin{bmatrix} 13.9308 & 8.6277 & 3.0391 & 4.6403 \\ 8.6277 & 27.3241 & 10.002 & 4.066 \\ 3.0391 & 10.002 & 23.9748 & 7.5937 \\ 4.6403 & 4.066 & 7.5937 & 21.2044 \end{bmatrix},$$

$$\mathbf{A} = \begin{bmatrix} 0 & 0 & 0 & 1 \\ 1 & 0 & 0 & 0 \\ 0 & 1 & 0 & 0 \\ 0 & 0 & 1 & 0 \end{bmatrix}, \quad k_c = 2, \quad b_i = \begin{cases} 1, & i = 1 \\ 0, & i \ne 1 \end{cases}, \tag{29}$$

where the matrix $\mathbf{P}$ is obtained by solving the linear matrix inequality described in ***Lemma 1***.

A. Continuous Communications

The secondary control in this case is as proposed in (10) with $k = 25$. Fig. 5 (a)-(b) depict the PCC bus voltage and DGs' output voltages. Prior to *t=1s*, the droop-control controls the MG leading to the deviation in the DG voltages and unregulated PCC voltage. After activating the secondary control at *t=1s*, DG voltages converge to a reference value which makes the PCC voltage regulated. At *t=4s*, the PCC load is doubled. Subsequently, the PCC voltage controller increases the reference voltage but not more than the allowable limit $(1.05V_{nom})$. Therefore, the DG voltages are set to $1.05V_{nom}$ and the PCC voltage remains as close as possible to V_{nom}. At *t=7s*, *load 2* and former added load to PCC load are switched off and the PCC voltage grows suddenly; therefore, PCC voltage controller decreases the reference voltage in order to regulate the PCC voltage.

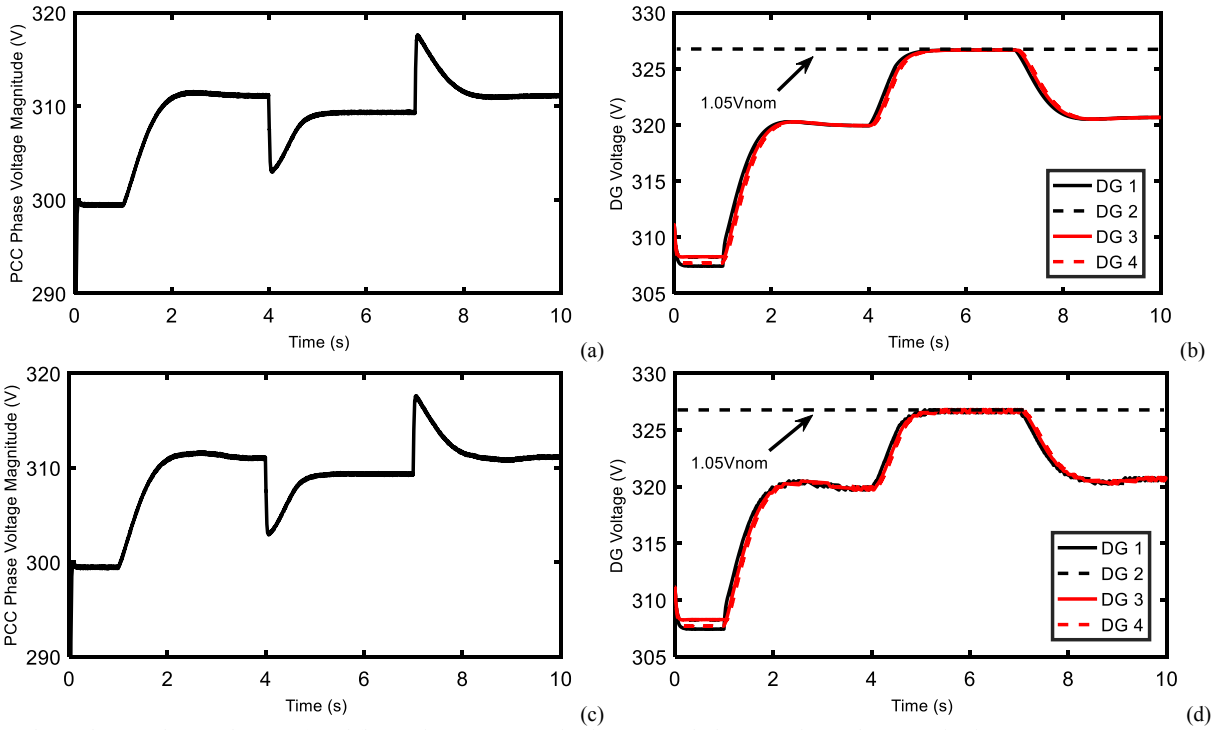

Fig. 5. PCC bus voltage and DG voltages: (a) and (b) continuous communications, (c) and (d) event-triggered communications.

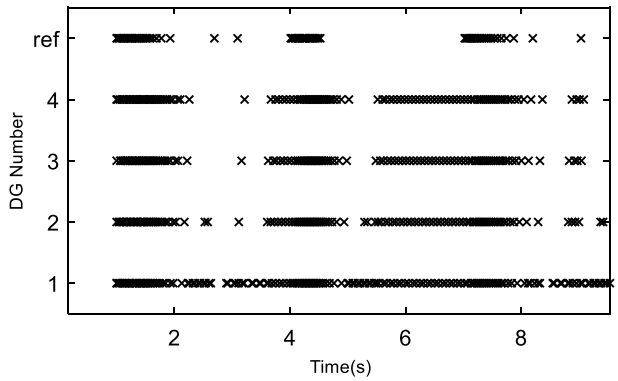

Fig. 6. Event-times associated with DGs and reference generator.

B. *Event-Triggered Communications*

Fig. 5 (c)-(d) depict the results for this case with $k = 25$ and $\Delta = \Delta_0 = 38720$. It is clear that as opposed to the former case, the DG voltage converge to the reference value with a nonzero error and have variation around the reference voltage. Fig. 6 depicts the event times associated with this case. It is shown that when the controller is activated at *t=1s*, DGs and reference generator start their communications until they converge to a steady state. They do not communicate significantly, until a load is changed. Subsequent to load change, they communicate again until they pass through this events. Therefore, one can see that the communication amount is adaptive to the load variations. The number of communications for reference generator and DGs 1 to 4 are 86, 189, 144, 137, and 139, respectively. Therefore, with a finite number of communications, we achieve a performance almost as in the former case. The minimum inter-event time is *2.734 ms*. As stated in the ***Remark 1*** and ***Remark 2*** the main objective in this paper is secondary voltage control. Therefore, DGs' frequencies and active powers are controlled by conventional droop-control and reactive power sharing is not addressed. Fig. 7 shows the variation of frequencies, active powers, and reactive powers associated with different DGs. It is shown that secondary controller activation at *t=1s* does not affect the frequency synchronization and active power sharing significantly. It is further shown that proper reactive power sharing and voltage regulation cannot be achieved simultaneously.

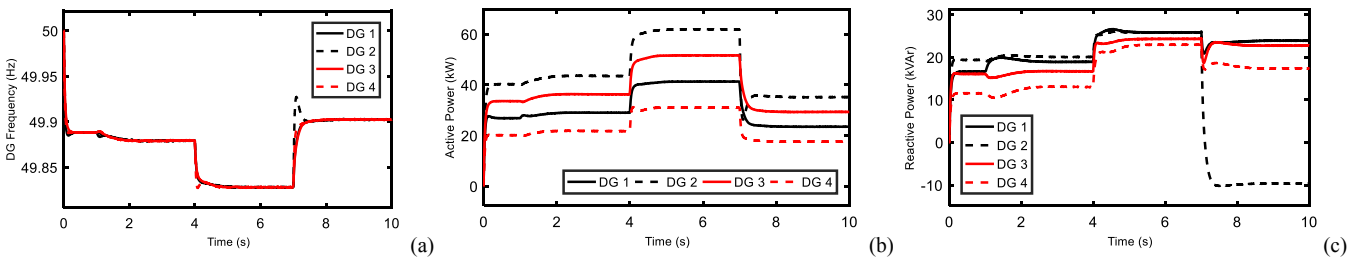

Fig. 7. (a) DG frequencies, (b) active powers, and (c) reactive powers under the proposed control scheme with event-triggered communications.

TABLE I. MINIMUM INTER-EVENT TIME (t_{min}) AND NUMBER OF COMMUNICATIONS FOR REFERENCE GENERATOR (*ref*) AND DGS 1 TO 4

Case ($\Delta_0 = 38720$)	t_{min}**(ms)**	**# of communications for DGs**				
		1	***2***	***2***	***4***	***ref***
$k = 25 \& \Delta = \Delta_0$	2.734	189	144	137	139	86
$k = 25 \& \Delta = 0.1\Delta_0$	0.865	372	337	323	339	266
$k = 50 \& \Delta = \Delta_0$	1.368	300	245	236	238	80

C. Event-triggered Communications for Different k & Δ

According to the ***Proof*** of ***Proposition 2***, parameters k and Δ determine the speed of convergence and its steady-state bound, respectively. Table I, summarizes the number of communications of DGs and reference generator, as well as the minimum inter-event time for different values of k and Δ. It is shown that, both greater k and smaller Δ, lead to more communications, as well as less minimum inter-event time.

V. CONCLUSION

A state-space model is developed for islanded MGs and is transferred to a multi-agent system with single integrator dynamics using feedback linearization technique. In order to restore the DG voltages to a reference value, a leader-following tracking control with both continuous and event-triggered communications is introduced. In addition, considering the voltage limits, a controller is designed for the critical bus voltage to track the nominal voltage. It is shown that the MG system with proposed event-triggered controller is *L_2-stable* and the inter-event times are always positive. Simulation results show the effectiveness of the proposed controllers.

REFERENCES

[1] J. M. Guerrero, M. Chandorkar, T.-L. Lee, and P. C. Loh, "Advanced control architectures for intelligent microgrids—Part I: Decentralized and hierarchical control," *IEEE Trans. Ind. Electron.*, vol. 60, no. 4, pp. 1254–1262, Apr 2013.

[2] M. Yazdanian and A. Mehrizi-Sani, "Distributed control techniques in microgrids," *IEEE Trans. Smart Grid*, vol. 5, no. 6, pp. 2901–2909, Nov 2014.

[3] S. Zuo, A. Davoudi, Y. Song, and F. L. Lewis, "Distributed Finite-Time Voltage and Frequency Restoration in Islanded AC Microgrids," *IEEE Trans. Ind. Electron.*, vol. 63, no. 10, pp. 5988–5997, Oct 2016.

[4] Q. Yang, J. A. Barria, and T. C. Green, "Communication infrastructures for distributed control of power distribution networks," *IEEE Trans. Ind. Informatics*, vol. 7, no. 2, pp. 316–327, May 2011.

[5] W. Heemels, K. H. Johansson, and P. Tabuada, "An introduction to event-triggered and self-triggered control," in *Decision and Control (CDC), 2012 IEEE 51st Annual Conference on*, Feb 2012, pp. 3270–3285.

[6] L. Dong, Y. Tang, H. He, and C. Sun, "An event-triggered approach for load frequency control with supplementary ADP," *IEEE Trans. Power Syst.*, vol. 32, no. 1, pp. 581–589, Jan 2017.

[7] W. Meng, X. Wang, and S. Liu, "Distributed load sharing of an inverter-based microgrid with reduced communication," *IEEE Trans. Smart Grid*, Jul 2016.

[8] Y. Fan, G. Hu, and M. Egerstedt, "Distributed Reactive Power Sharing Control for Microgrids With Event-Triggered Communication," *IEEE Trans. Control Syst. Technol.*, vol. 25, no. 1, pp. 118–128, Apr 2017.

[9] R. Han, N. L. D. Aldana, L. Meng, J. M. Guerrero, and Q. Sun, "Droop-free distributed control with event-triggered communication in DC micro-grid," in *Applied Power Electronics Conference and Exposition (APEC), 2017 IEEE*, May 2017, pp. 1160–1166.

[10] J. Zhou, H. Zhang, Q. Sun, D. Ma, and B. Huang, "Event-Based Distributed Active Power Sharing Control for Interconnected AC and DC Microgrids," *IEEE Trans. Smart Grid*, Jul 2017.

[11] Y. Cheng and V. Ugrinovskii, "Event-triggered leader-following tracking control for multivariable multi-agent systems," *Automatica*, vol. 70, pp. 204–210, Aug 2016.

[12] N. Pogaku, M. Prodanovic, and T. C. Green, "Modeling, analysis and testing of autonomous operation of an inverter-based microgrid," *IEEE Trans. power Electron.*, vol. 22, no. 2, pp. 613–625, Mar 2007.

[13] J. Schiffer, R. Ortega, A. Astolfi, J. Raisch, and T. Sezi, "Conditions for stability of droop-controlled inverter-based microgrids," *Automatica*, vol. 50, no. 10, pp. 2457–2469, Oct 2014.

[14] J.-J. E. Slotine and W. Li, *Applied nonlinear control*, vol. 199, no. 1. prentice-Hall Englewood Cliffs, NJ, 1991.

[15] A. Bidram, F. L. Lewis, and A. Davoudi, "Synchronization of nonlinear heterogeneous cooperative systems using input–output feedback linearization," *Automatica*, vol. 50, no. 10, pp. 2578–2585, Oct 2014.

[16] H. K. Khalil, *Noninear Systems*. Prentice-Hall, New Jersey, 1996.

[17] J. Hu and Y. Hong, "Leader-following coordination of multi-agent systems with coupling time delays," *Phys. A Stat. Mech. its Appl.*, vol. 374, no. 2, pp. 853–863, Feb 2007.